Acta Cryst. (1987). B43, 179-187

Effects of Crystal Packing and Hydration on the Conformation of Enniatin B

BY SHNEIOR LIFSON AND CLIFFORD E. FELDER

Department of Chemical Physics, Weizmann Institute of Science, Rehovot 76100, *Israel*

AND MAX DOBLER

*Laboratory for Organic Chemistry, Federal Institute of Technology (ETH), CH-*8092 *Zürich, Switzerland*

(*Received* 8 *July* 1985; *accepted* 11 *August* 1986)

Abstract

The effects of crystal packing forces and of hydration on the conformations of the ion carrier enniatin B, *cyclo*-{O–CH[–CH(CH_3)$_2$]–C′O′–N(CH_3)–CH[–CH(CH_3)$_2$]–C′O′–}$_3$, in two different crystal structures belonging to the trigonal space group $R3$ have been analyzed theoretically by the empirical force-field method. In one structure the central cavity of the ion carrier shrinks owing to crystal packing forces, while the c axis of the equivalent hexagonal unit cell is extended due to the presence of water molecules in the interlayer space. In the other crystal structure, a water molecule occupies the cavity and counterbalances the crystal packing forces, and therefore the observed molecular conformation resembles more closely the calculated conformation of the isolated single molecule than is the case for the first structure.

Introduction

Enniatin B (EnB) is a natural ion-carrier antibiotic, composed of three alternating residues each of D-hydroxyisovaleryl (D-HyIV) and L-*N*-methylvalyl (L-NMVal) linked into a cyclodepsipeptide by amide and ester bonds, according to the general formula

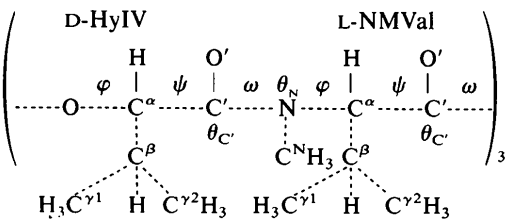

where φ, ψ and ω denote torsion angles, and $\theta_{C'}$ and θ_N denote out-of-plane angles (see Table 1). EnB binds ions by strong electrostatic interactions with the C′=O′ bond dipoles, and it carries the complexed ions through lipophilic membranes that interact favourably with the many CH_3 groups on the surface of EnB. Solution properties of EnB have been studied extensively by NMR, IR, CD, conductance, ultrasound and other methods, and reviewed extensively (Ovchinnikov, 1974; Burgermeister & Winkler-Oswatitsch, 1977; Ovchinnikov & Ivanov, 1982).

EnB is distinguished by its low binding selectivity, preferring K^+ mildly relative to Na^+, Rb^+ and Cs^+. This low selectivity has been commonly attributed to its 'conformational lability' that allows it to 'fit its cavity to the complexing ion' (Ovchinnikov, 1974). This interpretation was challenged by a detailed theoretical analysis of the conformations and energies of EnB and its alkali-ion complexes, using the empirical force-field method [Lifson, Felder & Shanzer, 1984, hereafter referred to as LFS(84)]. EnB was found to have a restricted flexibility, to be highly strained when an alkali ion is bound inside its cavity, and consequently to possess two competing modes of binding, internal and external. The larger ions prefer external binding, which does not depend on the geometry of the cavity, hence the low selectivity.

The most stable calculated conformation of EnB was compared by LFS(84) with the observed conformation then available from X-ray diffraction analysis (Tishchenko, Karimov, Vainshtein, Evstratov, Ivanov & Ovchinnikov, 1976) as part of a research program that linked theoretical and experimental tools in the design of synthetic biomimetic ion carriers (Lifson, Felder & Shanzer, 1983; Lifson, Felder, Shanzer & Libman, 1986). Some of the observed geometric parameters, particularly the very large out-of-plane angles of the amide and ester bonds (up to 24°), disagreed so much with the empirical force-field predictions that a need for a revision of the X-ray results was indicated. Indeed, such a revision [Tishchenko, Karaulov & Karimov 1982, hereafter referred to as TKK(82)] has been published, and its was gratifying to find a remarkable agreement between the revised conformation and the calculated one, as was pointed out in a note added in proof in LFS(84). However, the revised crystal structure [TKK(82)] was found to be hydrated. It belongs to the trigonal space group $R3$, with a C_3 crystallographic symmetry axis through the centre of the EnB molecule, and 1·5 water molecules along the threefold axis. One H_2O is at the molecular centre, while the other, with occupancy 0·5, is displaced by 2·6 Å toward the ester carbonyls.

0108-7681/87/020179-09$01.50

Another crystal structure investigation of EnB was cited in a review by Dobler (1981). This crystal structure [hereafter referred to as D(81)] also belongs to the trigonal space group $R3$, but its molecular conformation and unit-cell parameters are significantly different from those of TKK(82). A puzzling situation arose, since the D(81) crystal was believed to be unhydrated, yet it differed from the calculated unhydrated EnB structure in LFS(84), which resembled more the hydrated structure of TKK(82).

In D(81) the planes of the amide and ester groups are tilted obliquely to the mean plane of the ring, and the distances between the carbonyl O atoms on both sides of the EnB ring are less than 4·5 Å. In both the hydrated EnB [TKK(82)] and the calculated model [LFS(84)] these planes are practically perpendicular, and the corresponding carbonyl O distances are in the range 5·6–6·1 Å, thus forming a larger cavity. In addition, the slant, or shift, of the isopropyl groups of the HyIV and NMVal residues above and below the mean molecular plane, respectively, is more pronounced in D(81) than in the two other stuctures.

What is the origin of these differences? How are they related to intermolecular crystal packing forces? How are they affected by the presence of solvent traces in the crystal? The present theoretical investigation was undertaken to resolve these questions.

In the course of this investigation the crystal structure of D(81) was re-evaluated and refined, and the results were published recently [Kratky & Dobler, 1985, hereafter referred to as KD(85)]. The conformations of EnB according to D(81) and KD(85) are very similar. However, traces of a solvent molecule were observed in the refined structure. It was suggested that the solvent molecule was either MeOH or H_2O (the EnB crystals were grown in a mixture of MeOH and H_2O). In light of the present investigation, H_2O is the plausible choice.

Methods

Crystal energy calculations

The computer program used for the empirical force-field calculations (Lifson *et al.*, 1983, 1984) was augmented to include interactions with neighbouring molecules of a crystal by adding subroutines taken from program *MCA+QCPP/PI* (Huler, Warshel & Sharon, 1974; Huler, Sharon & Warshel, 1976; Warshel 1977). The Coulombic and Lennard-Jones 6-9 potential functions for the intermolecular interactions were the same as those employed in the intramolecular interactions, and were taken between each atom of the main molecule and each atom of its 24 nearest neighbours (see below). The energy was minimized simultaneously as a function of all the atomic coordinates of the main molecule, constrained to C_3 symmetry, and of the lattice unit-cell vectors, constrained to the trigonal $R3$ crystal system. All H atoms were represented explicitly. [Formerly, methyl groups had been represented as single 'extended atoms' (Lifson *et al.*, 1983, 1984), but this representation was found to be inadequate for crystal calculations.]

Treatment of crystal packing

The trigonal space group $R3$ was represented in terms of three unit-cell vectors comprising a C_3-symmetric system with respect to the molecular symmetry axis z, each of magnitude a and making an angle β with respect to this x axis. Thus, both molecular and lattice symmetries were utilized. First, the molecular conformation itself was minimized including a C_3 symmetry operator, as in LFS(84). Secondly, an asymmetric portion of the crystal structure, consisting of four molecules, represented an entire lattice region comprising 24 nearest neighbours of the central molecule (000). One molecule in the same hexagonal layer, $(1\bar{1}0)$ in the trigonal description, represented the six closest neighbours surrounding the central molecule, a second one in the next higher layer, (100), represented the six nearest neighbours in the layers above and below, a third one, $(11\bar{1})$, represented the six second-nearest neighbours in these two layers, and a fourth one, (110), represented the six nearest neighbours in the second-closest layers above and below the main molecule.

Water molecules

Since no H-atom coordinates were provided for the water molecules, these were estimated. For KD(85), they were positioned in a manner conducive to formation of hydrogen bonds to both adjacent amide O′ atoms and/or adjacent water molecules. Atom charges were estimated from the gas-phase dipole moment as O −0·66 and H 0·33. Since the water molecules of TKK(82) were located along the C_3 axis and one of them had an occupancy of only 0·5, in order to describe the situation adequately without loss of C_3 symmetry, they were represented as one or two parallel O–H dipoles lying along the C_3 axis, with partial atomic charges +/−0·41.

Results

We started our investigation with a simple 'computer experiment' designed to estimate the energy difference between the calculated equilibrium conformation and the observed one in D(81). If this value were small, crystal packing forces could account for the conformational change. This 'experiment' consisted of introducing fictitious energy functions for the φ and ψ torsion angles of both HyIV and NMVal residues, causing them to shift toward their values in

D(81). All other energy functions remained unchanged. The conformation obtained by minimizing the total energy of the system was expected to resemble the experimental one, since only φ and ψ are known to be highly flexible while all other internal coordinates are quite rigid. The resulting 'constrained φ, ψ' conformation is given in row 4 of Table 1. Other geometric and energetic parameters considered as significant measures for comparison are given in Table 2. The result of the experiment was encouraging: the total energy of the artificially restricted conformation was only 7·5 kJ mol^{-1} larger than that of the calculated equilibrium state. Such a small increase of molecular strain may be expected to be imposed by crystal packing forces. Furthermore, the restricted conformation resembled the experimental one more than the unrestricted equilibrium (see Table 1) and the size of the cavity at the centre of the molecule decreased as the carbonyl O atoms came closer to each other. This is the kind of conformational change which one would expect as a result of crystal packing forces that tend to minimize the volume of the crystal.

The computer experiment implied that crystal packing forces *could* account for differences between the observed crystal conformations of EnB and the calculated conformation of an isolated EnB molecule. In order to find out whether these forces *actually do* account for such differences we calculated the equilibrium conformation of the EnB molecule in the crystal by minimizing the energy of the unit cell as a function of all the molecular internal coordinates, as well as the unit-cell parameters and the orientation

Table 1. *Measured and calculated conformational angles of EnB* (°)

All conformations possess C_3 symmetry. See diagram in text for definitions of torsion angles. The out-of-plane angle $\theta_{C'}$ is defined as $\omega_1(O'\text{–}C'\text{–}X\text{–}C^{\alpha}) - \omega_2(C^{\alpha}\text{–}C'\text{–}X\text{–}C^{\alpha\prime}) + 180°$, where X is O for esters and N for amides. Similarly, $\theta_N = \omega_3(C^N\text{–}N\text{–}C'\text{–}C^{\alpha\prime}) - \omega_4(C^{\alpha}\text{–}N\text{–}C'\text{–}C^{\alpha\prime}) + 180°$.

	D-HyIV					L-NMVal			
	φ	ψ	$\theta_{C'}$	ω	θ_N	φ	ψ	$\theta_{C'}$	ω
(*a*) Unhydrated EnB									
D(81)[a]	81	−123	1	−168	18	−91	133	−1	174
Calc. crystal	90	−124	2	−178	−3	−92	126	−9	177
Calc. single molecule*	116	−104	1	−177	−2	−120	108	−3	178
Constrained φ, ψ†	78	−123	−5	−176	8	−84	130	14	174
(*b*) EnB.3H$_2$O									
KD(85)[b]	79	−125	6	−165	−5	−95	134	3	178
Calc. crystal (I)‡	88	−125	0	−173	−1	−91	123	−4	180
Calc. crystal (II)§	86	−125	2	−174	−2	−86	123	−6	178
Calc. single molecule	115	−106	0	−177	2	−118	108	3	178
(*c*) EnB.6H$_2$O									
Calc. crystal	73	−126	0	−175	−4	−74	128	5	173
Calc. single molecule	75	−132	−1	−174	3	−80	133	3	179
(*d*) EnB.1·5H$_2$O									
TKK(82)[c]	119	−110	1	−172	1	−120	107	0	176
Calc. no water	119	−96	1	−175	−4	−127	101	2	178
Calc. 1 O–H crystal¶	114	−110	0	−178	−7	−113	110	−4	177

References: (*a*) Dobler (1981); (*b*) Kratky & Dobler (1985); (*c*) Tishchenko, Karaulov & Karimov (1982).

* This same result is obtained from minimizing both KD(85) and TKK(92), as well as from the independent search for the conformation of lowest energy in LFS(84).

† See the 'computer experiment' in the *Results* section.

‡ The water hydrogen bonds to both adjacent amide O′ atoms with $H_w\cdots O'_{Hy} = 2·0$ and 1·9 Å.

§ The water hydrogen bonds to one adjacent amide O′ atom, $H_w\cdots O'_{Hy} = 2·2$ Å, and one adjacent water, $H_w\cdots O'_w = 2·0$ Å.

¶ The OH 'molecule' along the symmetry axis substitutes for the H_2O (occupancy = 1) that lacks C_3 symmetry. The O→H vector points towards the amide carbonyl atoms. Atom charges of H/O are +/−0·41. When H was put on the side of the ester carbonyl atoms, the O–H 'molecule' moved outside the molecular cavity during the minimization.

Table 2. *Geometric parameters (distances in* Å, *angles in* °) *and crystal packing energies* (kJ mol^{-1}) *for measured and calculated conformations of EnB*

The various conformations listed are identified in Table 1. The abbreviations O_{Va} and O_{Hy} refer to the NMVal and HyIV residues, respectively.

	Interatomic distances			Tilt angle*		^{i}Pr	Crystal packing energy‡		
	$O'_{Va}\cdots O'_{Va}$	$O'_{Hy}\cdots O'_{Hy}$	$C^N\cdots C^N$	Esters	Amides	$\Delta z(C^{\beta})$†	Str.	Hydr.	Latt.
(*a*) Unhydrated EnB									
D(81)	4·52	4·09	6·01	−16·3	−24·1	2·06	—	—	—
Calc. crystal	5·15	4·81	6·60	−15·0	−18·7	2·02	22·2	—	−243.7
Calc. single molecule	6·13	5·88	5·48	7·0	3·6	1·68	0·0	—	—
Constrained φ, ψ	4.80	4·67	6·01	−27·6	−22·0	2·12	7·5	—	—
(*b*) EnB.3H$_2$O									
KD(85)	4·39	4·30	6·13	−20·7	−20·7	2·20	—	—	—
Calc. crystal (I)	5·22	4·41	6·71	−12·0	−22·2	2·19	26·0	−87·9	−265·4
Calc. crystal (II)	5·15	4·39	6·82	−13·5	−24·4	2·28	25·1	−87·9	−266·7
Calc. single molecule	6·17	5·70	5·55	6·6	0·9	1·70	0·42	−90·9	—
(*c*) EnB.6H$_2$O									
Calc. crystal	4·37	4·23	7·20	−24·0	−27·2	2·71	84·5	−134·8	−298·1
Calc. single molecule	4·54	4·14	7·11	−23·9	−30·9	2·15	46·9	−128·1	—
(*d*) EnB.1·5H$_2$O									
TKK(82)	5·79	5·61	5·16	4·5	3·9	1·70	—	—	—
Calc. no water	6·24	6·21	4·73	10·1	12·2	1·80	11·3	—	−250·4
Calc. 1 O–H crystal	6·01	5·63	5·50	3·7	3·0	1·75	17·2	−35·6	−258·3

* The tilt angle is defined as the angle between the z axis of molecular C_3 symmetry and the mean plane through the atoms that form the ester or amide group.

† $\Delta z(C^{\beta})$ is defined as the z component of the distance (Å) between the C^{β} atoms for two adjacent isopropyl sidechains.

‡ Calculated relative to the uncomplexed single molecule. The three components given are Str., the conformational strain energy of the EnB molecule; Hydr., the hydration energy of the EnB molecule by the water molecule(s) hydrogen bonded to it; and Latt., the interaction energy of the central unit cell (including water) with the 24 nearest-neighbour unit cells.

of the molecule in the unit cell. Included in the energy function were all intramolecular interactions as well as all intermolecular interactions between the molecule in the central unit cell and all its 24 nearest neighbours (see *Methods* section.) In all crystal equilibrium calculations we used the experimental crystal coordinates as the initial values for energy minimization. Several models were calculated and the reasons for choosing them will be discussed in the next section. Table 1 presents the torsion and out-of-plane angles of the EnB ring for the various measured and calculated conformations. The experimental and calculated Cartesian coordinates are presented concisely in the scaled drawings given in the *xy* and *xz* projections (Figs. 1*a*,*b*–5*a*,*b*). The stereoviews (Figs. 1*c*–4*c*) complement the information in the tables and the scaled drawings. Table 2 presents the geometric parameters, which are the clearest manifestations of the effects of crystal packing and hydration on the EnB conformation. It also includes the energies of molecular strain, hydration and intermolecular interactions that together form the total crystal packing energy. Table 3 lists the trigonal *R*3 and equivalent hexagonal unit-cell parameters, as well as the orientation of the molecule in the unit cell and the unit-cell volume. Tables 4 and 5 present the short contact distances between atoms in the same layer and in adjacent layers, respectively.

Discussion

Two questions were posed in the introduction: (*a*) Do the differences between the conformations of the EnB molecule in isolation and in the crystal originate from the intermolecular packing forces in the crystal? (*b*) How does the incorporation of solvent molecules in the crystal affect the crystal structure?

We consider the first question by comparing the unhydrated molecule and the unhydrated crystal with one another, as well as comparing both with the experimental structure, starting with the crystal of D(81) and KD(85). The data for comparison are presented in the first part of the tables, labelled 'unhydrated EnB'. Initially, the coordinates for the minimization of the energy of the calculated crystal were the experimental coordinates of D(81), but the refined KD(85) coordinates led to the same calculated crystal structure. Examination of Table 1 shows that the conformation of EnB in the calculated crystal differs considerably from that of the calculated single molecule, the difference being due, of course, to the effect of the crystal forces. It shows also that EnB in the calculated crystal resembles the experimental KD(85) crystal more than the calculated single molecule of EnB. Table 2 demonstrates that crystal forces act in the direction of reducing the size of the cavity at the centre of EnB. The tilt angles of both esters and amides shift from positive values in the single molecule (*i.e.* carbonyls pointing away from the symmetry axis) to negative values close to the experimental ones. The carbonyl O distances decrease by about 1 Å, coming more than halfway towards the corresponding experimental distances.

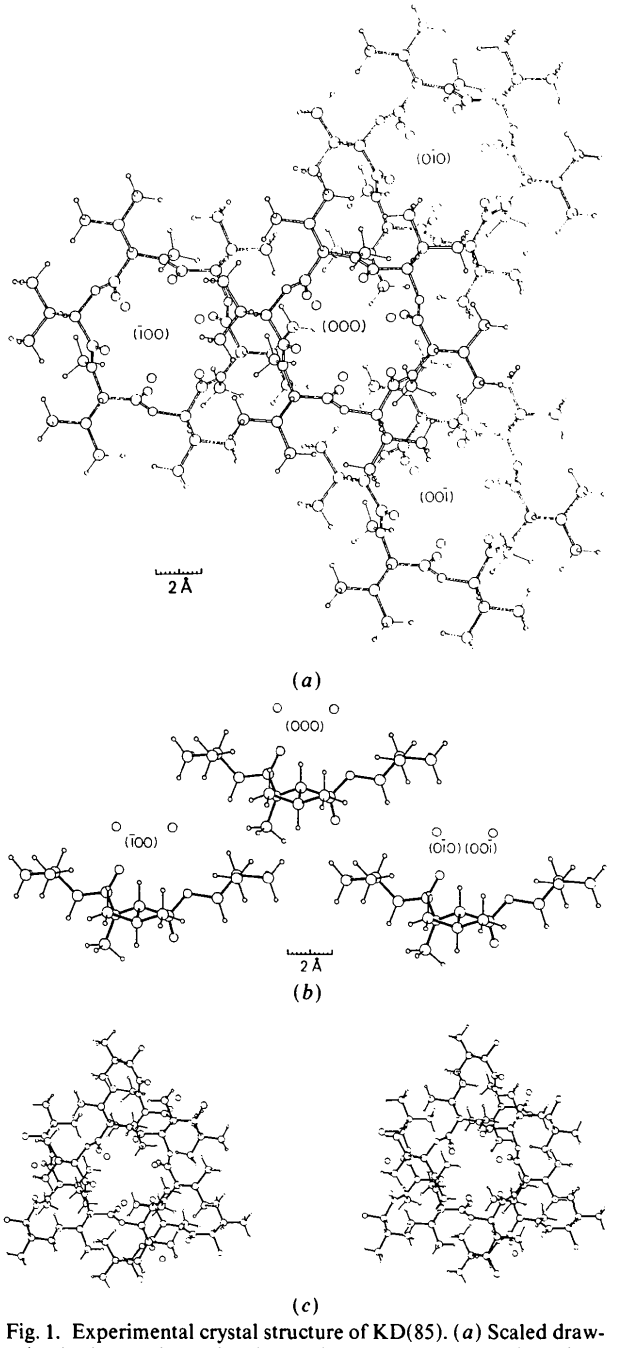

Fig. 1. Experimental crystal structure of KD(85). (*a*) Scaled drawing in the *xy* plane, showing a trigonal *R*3 representation of the central EnB molecule (000) and the three nearest neighbours in the next layer below: ($\bar{1}$00), (0$\bar{1}$0) and (00$\bar{1}$). (*b*) Scaled drawing in the *yz* plane of a section of EnB between two C^{α}_{HyIV} atoms for molecules (000), (0$\bar{1}$0) and (00$\bar{1}$). The three Cartesian coordinates of all atoms can be read off using (*a*) for *x* and *y* and (*b*) for *z*. The scale represents 2 Å, ruled off in 0·2 Å units. (*c*) Stereoview in the *xy* plane.

The description given above, of the conformation of EnB in KD(85) being derived from that of the single EnB molecule by contraction of the cavity due to crystal packing forces, is supported by other observations from Table 2. The tilt of the carbonyls inward cannot be effected without shifting the isopropyl groups away from the molecular plane. This is represented by the projection $\Delta z(C^{\beta})$ of the distance between adjacent C^{β} atoms along the symmetry axis, and indeed the observed shift in the refined crystal structure [KD(85); 2·2 Å] as well as in the calculated crystal structures (2·2, 2·3 Å) is larger than in the single EnB molecule (1·7 Å). Moreover, contraction of the cavity is energetically feasible, since the strain energy accompanying the EnB contraction is about an order of magnitude smaller than the lattice energy, although it is three times as large as that of the 'constrained φ, ψ' single molecule.

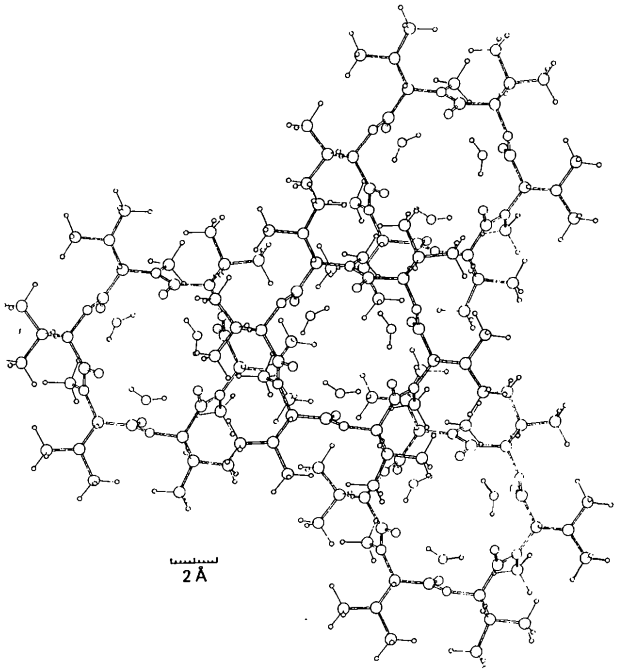

(*a*)

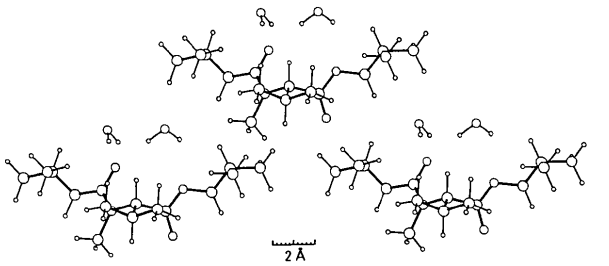

(*b*)

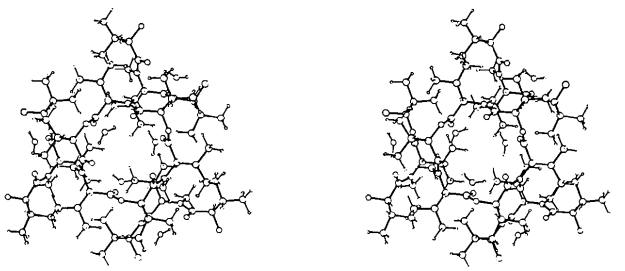

(*c*)

Fig. 2. Calculated crystal structure of EnB.3H$_2$O (I): (*a*)-(*c*) as in Fig. 1.

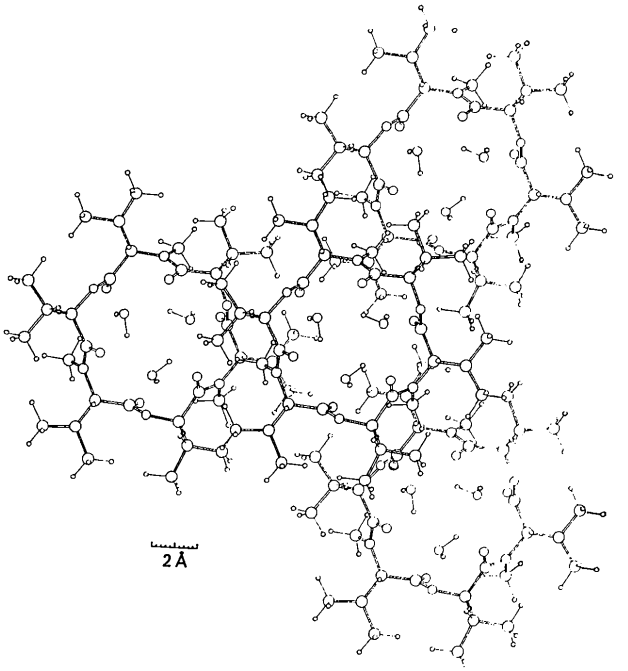

(*a*)

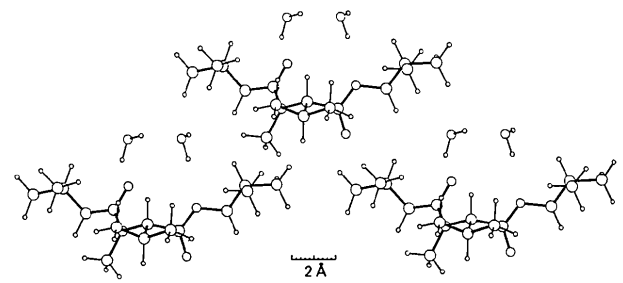

(*b*)

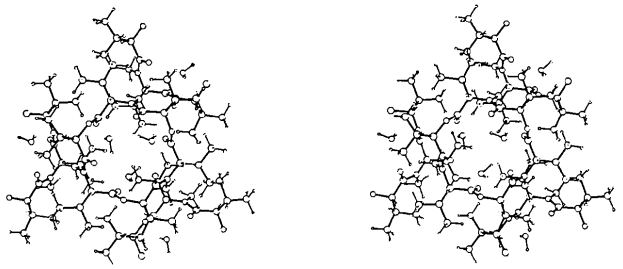

(*c*)

Fig. 3. Calculated crystal structure of EnB.3H$_2$O (II): (*a*)-(*c*) as in Fig. 1.

At this point it is interesting to compare both the LFS(84) single molecule and the KD(85) crystal with the TKK(82) hydrated EnB.1·5H_2O, represented in the last part of Tables 1-3. Since in this crystal the molecule contains a water molecule at the centre of its cavity, it cannot shrink, and therefore its molecular conformation is expected to resemble that of the single molecule. Indeed, this resemblance can be recognized in the φ and ψ angles of Table 1 and in all geometric parameters of Table 2.

The $\Delta z(C^\beta)$ values of Table 2 correlate well with the unit-cell parameters of Table 3. In the TKK(82) crystal, Δz is smaller than in the KD(85) crystal, namely the isopropyls are shifted by a smaller amount, and as a result the hexagonal axis a is larger, and c is smaller. However, the difference in a is only 0·37 Å while that in c is 1·74 Å. Consequently, the unit-cell volume per molecule of the EnB.1·5H_2O crystal is 7% smaller than KD(85), although the latter's cavity has shrunk considerably, as we have seen already.

These apparently contradictory trends are fully accounted for by assuming that the KD(85) crystal is hydrated. The consequences of this assumption are presented in Tables 1-3 under the heading 'EnB.3H_2O'. The calculated values of the hexagonal unit-cell parameter c of EnB.3H_2O in both its hydrated forms (I) (15·96 Å) and (II) (16·08 Å) shift away from that of the calculated unhydrated EnB (15·19 Å) and are closer to that of the experimental KD(85) crystal (16·31 Å). The calculated volume of

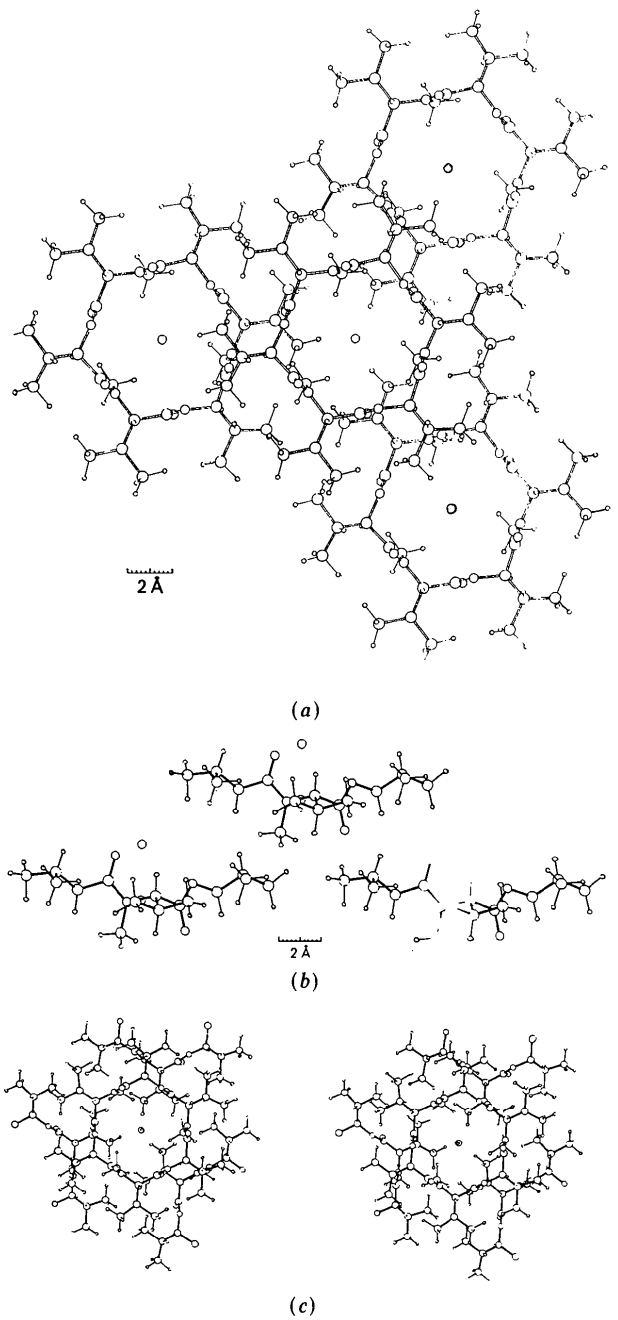

Fig. 4. Experimental crystal structure of TKK(82): (*a*)-(*c*) as in Fig. 1.

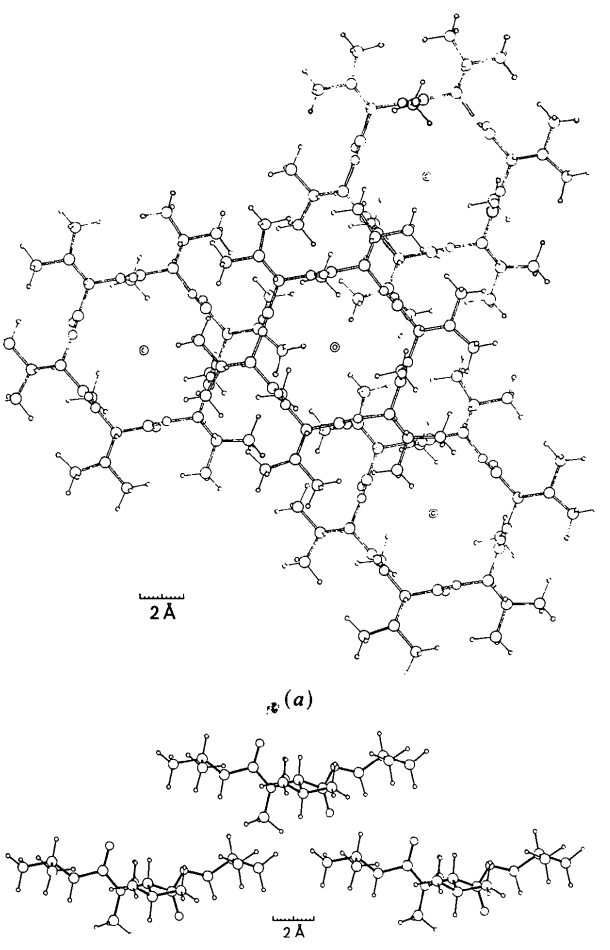

Fig. 5. Calculated crystal structure of EnB.1O–H: (*a*), (*b*) as in Fig. 1.

Table 3. *Crystallographic unit-cell parameters* (Å) *and orientation for measured and calculated conformations of EnB*

The various conformations listed are identified in Table 1.

	Trigonal $R3$ parameters		Equivalent hexagonal parameters		Orientation angle* (°)	Cell volume (Å^3)
	a	α	a	c		
(a) Unhydrated EnB						
D(81)	10·031	93·65	14·63	16·26	8·56	1005
Calc.	9·929	96·32	14·80	15·19	11·12	960
(b) EnB.3H_2O						
KD(85)	10·043	93·47	14·63	16·31	9·98	1007
Calc. (I)	10·047	94·54	14·76	15·96	9·91	1004
Calc. (II)	10·042	94·15	14·71	16·08	11·22	1004
(c) EnB.6H_2O						
Calc.	10·190	90·05	14·42	17·63	8·49	1055
(d) EnB.1·5H_2O						
TKK(82)	9·921	98·2	15.00	14·52	33·26	943
Calc. no water	9·928	98·87	15·08	14·30	33·49	939
Calc. 1 O–H	9·900	98·25	14·97	14·48	32·26	936

* The orientation angle is defined as follows: Let a be one of the unit-cell vectors in the trigonal $R3$ representation. Let P_a be the projection of a onto the xy plane perpendicular to the molecular symmetry axis z. Let P_C, similarly be the projection of the vector location of the nearest ester carbonyl C atom C′. The orientation angle is the angle between these two projections.

Table 4. *Interatomic contact distances* (Å) *between neighbouring molecules in the same layer: measured and calculated EnB crystals*

Distances greater then 4·2 Å are represented by an asterisk. The various conformations listed are identified in Table 1. The abbreviations C_{Hy} and C_{Va} refer to HyIV and NMVal residues, respectively.

	$C^{\gamma 1}_{Va}$–$C^{\gamma 2}_{Va}$	$C^{\gamma 2}_{Va}$–$C^{\gamma^2}_{Hy}$	$C^{\gamma 1}_{Hy}$–$C^{\gamma 1}_{Va}$	$C^{\gamma 1}_{Hy}$–$C^{\gamma 2}_{Hy}$
(a) Unhydrated EnB				
D(81)	4·0	3·5	*	3·8
Calc.	3·6	3·4	*	3·9
(b) EnB.3H_2O				
KD(85)	3·8	3·5	*	4·0
Calc. (I)	3·6	3·5	*	4·0
Calc. (II)	3·7	3·4	*	4·1
(c) EnB.6H_2O				
Calc.	3·5	3·5	*	4·0
(d) EnB.1·5H_2O				
TKK(82)	4·1	*	3·7	3·9
Calc. no water	4·0	*	3·8	3·7
Calc. 1 O–H	4·0	*	3·6	3·7

the EnB.3H_2O crystal is 1004 Å^3, in excellent agreement with the experimental value of KD(85) (1007 Å^3), while the calculated unit-cell volumes of the KD(85) and TKK(82) crystals, when both are assumed to be unhydrated, are 960 and 939 Å^3, respectively, both very close to the experimental value of TKK(82) (943 Å^3).

The electron-density peak observed in the refined structure of KD(85) and interpreted as an O atom was suggested to represent either water or methanol (the crystals were grown in a water/MeOH mixture). That it is indeed H_2O, and that it accounts for the excess volume noted above, is seen from its position within the lattice, presented to scale in Figs. 1(a,b), and in a stereoview (Fig. 1c). As it is located off the C_3 symmetry z axis, it occupies three positions near the EnB molecule, at a distance of about 3 Å from two adjacent amide carbonyl O atoms (O′), and forms an angle of 134° with them. It is therefore natural to assume that the solvent molecule is H_2O, hydrogen bonded to the two carbonyls. The measured density (KD85) $D_m = 1.13$ g cm^{-3} allows for 2·3H_2O molecules per unit cell, namely one per asymmetric unit, with occupancy 0·77, but the accuracy of the structure determination does not exclude full occupancy. Since our computational methods do not allow for partial occupancies, we calculated the crystal structure as EnB.3H_2O, starting from the experimental coordinates of the refined structure [KD(85)]. Two forms of hydration were found to be consistent with the experimental data, and to be equally probable since they possess about the same total energy. They are denoted (I) and (II) (Figs. 2, 3). In (I), the water H atoms bond to both adjacent O atoms of the amide carbonyls. In (II), one H bonds to a carbonyl O atom while the other bonds to the O of a neighbouring H_2O molecule. To complete the theoretical description, and to distinguish between hydration and crystal packing effects, we also calculated these two forms of the hydrated single EnB molecule. It was found to prefer the hydrogen-bonding pattern of crystal (II). Table 1 shows that the hydrated and unhydrated EnB conformations in the crystal resemble each other, and the same is true for the single molecule, while the conformation in the crystal differs significantly from the single molecule in both hydrated and unhydrated cases. However, Table 2 indicates a definite effect of the hydration on the amide groups. The amide O distances come close to the experimental values as a result of the H_2O–amide O interactions, and the tilt of the amide group is also increased by the hydration. Note that the hydration of the single molecule alone produces neither the amide O distances nor the amide tilt observed in the experimental lattice, and that the lattice energy is about three times larger than the hydration energy. Thus it may be concluded that the molecular conformation is affected by crystal forces more than by H_2O–EnB interactions.

A more detailed presentation of the role of the three water molecules in increasing the interlayer distance by being intertwined between the layers is given by the interatomic contact distances between neighbouring molecules in the same layer and in adjacent layers in Tables 4 and 5, respectively. Contact distances are obtained as the sum of van der Waals radii, assumed to be 2·0 Å for the methyl group and 1·5 Å for oxygen (Pauling, 1960). Tables 4 and 5 represent all methyl–methyl distances <4·0 Å and all O–methyl distances <3·8 Å. For the sake of comparison, when two atoms form a contact in one structure, their distance is given in all other structures up to a limit of 4·2 Å. Larger distances are represented by an asterisk.

Table 5. *Interatomic contact distances (Å) between neighbouring molecules in adjacent layers; measured and calculated EnB crystals*

Distances greater than 4·2 Å are represented by an asterisk. The various conformations listed are identified in Table 1. The abbreviations C_{Hy} and C_{Va} refer to HyIV and NMVal residues, respectively. O_w is a solvent or water O atom.

Central molecule	C^{α}_{Va}	$C^{\gamma 2}_{Va}$	$C^{\gamma 1}_{Hy}$	$C^{\gamma 1}_{Hy}$	$C^{\gamma 2}_{Hy}$	$C^{\gamma 2}_{Hy}$	$C^{\gamma 2}_{Hy}$	$C^{\gamma 2}_{Hy}$	O'_{Hy}	O_w	O_w	O_w	O_w	O_w
Neighbour molecule	C^{N}_{Va}	C^{N}_{Va}	C^{β}_{Va}	$C^{\gamma 2}_{Va}$	C^{β}_{Va}	$C^{\gamma 1}_{Va}$	$C^{\gamma 2}_{Va}$	O'_{Va}	C^{N}_{Va}	C^{N}_{Hy}	C^{α}_{Hy}	C^{β}_{Hy}	$C^{\gamma 1}_{Hy}$	$C^{\gamma 2}_{Hy}$
(*a*) Unhydrated EnB														
D(81)	3·9	*	*	4·0	*	*	*	*	4·0	—	—	—	—	—
Calc.†	3·6	3·9	3·9	3·8	4·0	*	4·0	3·5	3·4	—	—	—	—	—
(*b*) EnB.3H_2O														
KD(85)	4·0	4·2	4·1	4·0	4·0	4·0	*	3·8	3·9	3·7	3·7	3·8	3·5	3·7
Calc. (I)	3·9	4·1	3·8	3·8	4·1	4·0	*	3·4	3·6	3·4	3·7	3·8	3·6	3·6
Calc. (II)	3·9	*	3·8	3·8	4·1	4·0	*	3·4	3·6	3·7	3·9	3·9	3·6	3·6
(*c*) EnB.6H_2O														
Calc.‡	*	*	4·0	3·7	4·0	3·8	*	3·9	3·8	3·2	4·0	*	4·0	4·0
Central molecule	$C^{\gamma 2}_{Va}$	C^{β}_{Hy}	C^{β}_{Hy}	$C^{\gamma 1}_{Hy}$	$C^{\gamma 2}_{Hy}$	$C^{\gamma 2}_{Hy}$	C'_{Hy}	C^{α}_{Va}	$C^{\gamma 1}_{Va}$	$C^{\gamma 2}_{Va}$	O'_{Hy}	O'_{Hy}	O'_{Hy}	O'_{Hy}
Neighbour molecule	C^{N}_{Va}	C^{N}_{Va}	$C^{\gamma 1}_{Va}$	C^{N}_{Va}	C^{β}_{Va}	$C^{\gamma 1}_{Va}$	C^{N}_{Va}	O'_{Va}	O'_{Va}	O'_{Va}	C^{N}_{Va}	O'_{Va}	C^{α}_{Hy}	$C^{\gamma 1}_{Hy}$
(*d*) EnB.1·5H_2O														
TKK(82)	3·8	*	4·2	3·7	4·0	4·0	*	3·8	3·6	3·9	3·7	3·8	3·8	3·6
Calc. no water§	3·6	*	3·9	3·8	4·0	3·8	*	3·6	3·7	3·8	3·6	3·6	3·7	3·8
Calc. 1 O–H	3·7	4·1	4·0	3·5	4·0	3·8	4·1	3·7	3·8	3·7	3·5	3·8	3·8	3·8

† Contains in addition the contact $C^{\gamma 2}_{Hy}$–$C^{\gamma 2}_{Va}$ = 4·0 Å.
‡ Contacts of the three additional O_w to: C^{β}_{Va} = 3·9, $C^{\gamma 1}_{Va}$ = 3·6, $C^{\gamma 2}_{Va}$ = 3·5, and $C^{\gamma 2}_{Hy}$ = 4·1 Å.
§ Contains in addition the contact $C^{\gamma 1}_{Hy}$–C^{β}_{Va} = 4·0 Å..

The interatomic contacts within a layer (Table 4) are few but rather short; in particular, there is the short oblique contact in the EnB.3H_2O lattice between $C^{\gamma 2}_{Va}$ located below the molecular plane and $C^{\gamma 2}_{Hy}$ located above the plane. The repulsion between these methyl groups is the cause of the tilts of the isopropyl groups resulting in the increase of $\Delta z(C^{\beta})$ in Table 2.

The interatomic contacts in adjacent layers are distributed about equally between methyl–methyl and O–methyl contacts in both KD(85) and TKK(82) crystals. However, while in KD(85) five out of seven O contacts are with water, all such contacts in TKK(82) are made by the carbonyl O atoms. The unhydrated model is seen to have too few contacts to maintain the crystal packing, thus further supporting the suggestion that the KD(85) crystal is indeed hydrated.

A model of an EnB.6H_2O hydrated crystal is also included in Tables 1–5. Its purpose was to examine the effect of hydration of both amide and ester carbonyls. The results are perhaps interesting but inconclusive. This model brings the calculated ester carbonyl distances of the KD(85) crystal (Table 2) closer to the observed values, but many other parameters are shifted away from their observed values. The augmented hydration is also less probable energetically, since the three added water molecules contribute about 40 kJ mol^{-1} to the hydration, half as much as the first three. If the hydration of the KD(85) crystal were based on partial occupancy, some ester carbonyl–water interactions would be conceivable, but further clarification requires more experimental work on better crystals.

In comparing theory and experiment it is important to recognize and evaluate both points of agreement and disagreement. We therefore now comment on the main discrepancies between the calculated and observed data. Most such discrepancies originate presumably from inaccuracies, partly related to energy parameters of the force field [LFS(84)], and partly concerning difficulties in obtaining better crystal data [KD(85)].

The calculated contact distances are, on the average, somewhat shorter than the observed ones (Tables 4 and 5), and this is expressed in slightly shorter calculated unit-cell parameters (Table 3). There are also puzzling differences between some calculated and observed conformational parameters. For example, the observed amide bond in EnB.3H_2O is twisted out of planarity ($\omega = -165°$, Table 1) twice as much as the calculated bonds (-173, $-174°$); differences of about 10° occur in some other torsion angles as well. The calculated distance between the ester carbonyl O atoms in EnB.3H_2O is longer by about 0·8 Å than the observed distance (Table 2). Further optimization of the empirical force-field energy parameters may perhaps improve the agreement between calculated and observed values. However, such improvements cannot be made within the data of one molecular system, but must fit the properties of other molecules consistently. This is obviously beyond the scope of the present study, and is also not relevant for the present purpose.

Notwithstanding the questions left open for further research, the general agreement between theory and experiment as presented in this study strongly supports the answers given to the questions raised in the introduction. The differences between the conformations and unit-cell parameters of the two observed EnB crystals, as well as the differences between these and the calculated single EnB molecule, are reasonably accounted for by the effects of crystal packing

forces, and by the different forms of hydration of these crystals.

References

BURGERMEISTER, W. & WINKLER-OSWATITSCH, R. (1977). In *Topics in Current Chemistry* 69, *Inorganic Biochemistry* II. Berlin: Springer-Verlag.

DOBLER, M. (1981). *Ionophores and Their Structures.* New York: John Wiley.

HULER, E. H., SHARON, R. & WARSHEL, A. (1976). Quantum Chemistry Program Exchange, 325.

HULER, E. H., WARSHEL, A. & SHARON, R. (1974). *MCA+ QCPP/PI.* Weizmann Institute Department of Chemical Physics, Rehovot.

KRATKY, C. & DOBLER, M. (1985). *Helv. Chim. Acta*, **68**, 1798-1803.

LIFSON, S., FELDER, C. E. & SHANZER, A. (1983). *J. Am. Chem. Soc.* **105**, 3866-3875.

LIFSON, S., FELDER, C. E. & SHANZER, A. (1984). *Biochemistry*, **23**, 2577-2590.

LIFSON, S., FELDER, C. E., SHANZER, A. & LIBMAN, J. (1986). In *Progress in Macrocyclic Chemistry*, Vol. 3, *Synthesis of Macrocycles: The Design of Selective Complexing Agents*, edited by R. M. IZATT & J. J. CHRISTENSEN. New York: John Wiley.

OVCHINNIKOV, Y. A. (1974). *FEBS Lett.* **44**, 1-21.

OVCHINNIKOV, Y. A. & IVANOV, V. T. (1982). In *The Proteins*, 3rd ed., Vol. V, edited by Y. H. NEURATH & R. L. HILL. New York: Academic Press.

PAULING, L. (1960). *The Nature of the Chemical Bond*, 3rd ed. p. 260. Cornell Univ. Press.

TISHCHENKO, G. N., KARAULOV, A. I. & KARIMOV, Z. (1982). *Cryst. Struct. Commun.* **11**, 451-456.

TISHCHENKO, G. N., KARIMOV, Z., VAINSHTEIN, B. K., EVSTRATOV, A. V., IVANOV, V. T. & OVCHINNIKOV, Y. A. (1976). *FEBS Lett.* **65**, 315-318.

WARSHEL, A. (1977). *Comput. Chem.* **1**, 195-202.

Acta Cryst. (1987). B**43**, 187-197

Diffuse Scattering and Disorder in Urea Inclusion Compounds $OC(NH_2)_2+C_nH_{2n+2}$

BY R. FORST, H. JAGODZINSKI, H. BOYSEN AND F. FREY

Institut für Kristallographie und Mineralogie, 8000 *München* 2, *Theresienstrasse* 41, *Federal Republic of Germany*

(*Received* 21 *February* 1986; *accepted* 21 *August* 1986)

Abstract

Diffuse scattering phenomena in urea inclusion compounds with hexadecane and dodecane adducts were investigated by X-ray and neutron diffraction methods from 380 down to 32 K. In the four different phases of the compound with hexadecane, more than six different kinds of diffuse scattering are found. Most intense are two diffuse layer-line systems perpendicular to the pseudo-hexagonal c^* axis with periods which are incommensurate with the Bragg layers which correspond to the averaged structure. Within these diffuse layers short-range-order maxima were observed. Strong Bragg reflections are accompanied by diffuse wings parallel to $\mathbf{c}^*$. Wavy diffuse streaks parallel to the $\mathbf{a}^*\mathbf{b}^*$ plane connect the Bragg reflections. A critical increase of diffuse scattering occurs as a precursor of superstructure reflections approaching the phase transition II → III from above. A semi-quantitative interpretation of the diffuse layers is given in terms of longitudinal and lateral ordering/disordering of the paraffin chains within the urea framework. The wavy streaking may be understood as interfacial scattering. A complicated satellite pattern in the low-temperature phase (< 120 K) is analysed in terms of a domain structure caused by competing ordering forces within the paraffin-chain system and between host and guest.

0108-7681/87/020187-11$01.50

I. Introduction

Urea inclusion compounds may be characterized by a framework of urea with open channels along a unique (**c**) axis exhibiting a honeycomb-like cross section. Within these channels chains consisting of *n*-alkane molecules C_nH_{2n+2} are embedded. There are simple arguments against the naive assumption that the *n*-alkanes are nothing but weakly bound guests in a practically unaltered host (= urea) structure as in the case of zeolite or clathrate inclusion structures: pure urea crystallizes in a completely different (tetragonal) structure as compared with the adduct compound where it has - on average - a hexagonal symmetry (high-symmetry phase). The hexagonal framework collapses by decomposition several degrees below the melting point of pure urea (McAdie, 1962). The inclusion therefore stabilizes the framework, indicating remarkable interaction forces between host and guest. In addition there are direct interactions between the chain molecules in longitudinal (*i.e.* parallel to **c**) and lateral (perpendicular to **c**) directions. These competing temperature-dependent interactions are responsible for the occurrence of different phases and a variety of disorder phenomena which manifest themselves by more or less complicated diffraction patterns (Lenné, 1963; Lenné, Mez & Schlenk, 1970; Forst, 1984).